Quantum Mechanical Modeling Techniques for High-Performance Low-k Amorphous Material Engineering: a Showcase for aBN

Blanka Magyari-Köpe[1], Hans Hsu[2], and Jeff Wu[2]
[1]Taiwan Semiconductor Manufacturing Company Technology Inc., San Jose, CA, USA, email: blankamk@tsmc.com
[2]Taiwan Semiconductor Manufacturing Company Ltd., Hsinchu, TW

Abstract—As technology continues to advance, the semiconductor industry is constantly on the lookout for new materials that are both high-performing and cost-effective. One promising avenue for achieving further gains is through the use of amorphous materials with desirable properties that can be incorporated in semiconductor processing steps. To optimize these materials, advanced and efficient material simulation techniques are needed to address the complex nature of bonding and structural effects, predict, and analyze their properties, and provide suitable engineering solutions. This paper highlights a novel approach for studying the behavior of low-k amorphous materials under repetitive structural pulses that can be applied in any future amorphous material study. By efficiently capturing important experimental data, such as atomic density ranges, compositions, porosities, and dielectric constants, the method provides valuable insights that cannot be obtained through experimentation alone. Additionally, the paper includes a discussion on segregation trends and addresses effects of impurities as possible knobs for further optimization and material engineering.

I. INTRODUCTION

Amorphous materials play a vital role in semiconductor industry due to their distinctive electronic, optical, and mechanical properties. With the increasing demand for high-performance, cost-effective materials compatible with miniaturization processes, the importance of amorphous materials has further amplified over the past decade. Among the most promising applications, low-k dielectric material development [1-3] is crucial for continued scaling of electronic devices as reduces parasitic capacitance between conducting wires, leads to optimized power consumption and improves overall performance. Despite significant previous efforts, the development of new amorphous materials still faces substantial challenges due to complexities in optimizing growth processes and treatment conditions at high temperatures, pressures, and operations at high electric fields. To overcome these challenges and obtain effective solutions, atomic-level insight is required by advanced quantum mechanics based atomistic modeling techniques [4] to provide accurate descriptions of material structures and dynamics, enable identification of atomic scale mechanisms that govern film formation, which are perspectives difficult or impossible to attain from experiments alone.

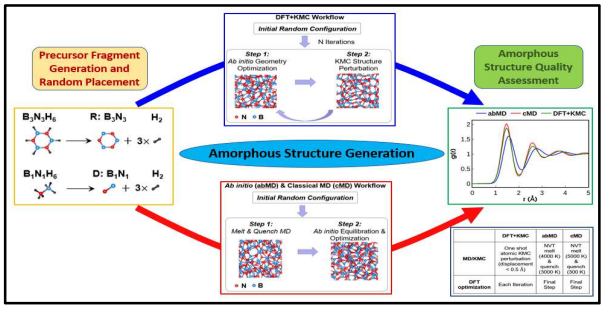

Fig. 1. Pulse-like perturbations by DFT+KMC, *ab initio* and classical MD on randomly placed precursor fragments produce similar quality amorphous structures by average radial distribution function analysis.

To accurately model amorphous thin films, however, atomistic simulations must account for coexistence profiles of metastable local regions on the potential energy surface (PES) and provide thermodynamic stability assessments, besides bonding patterns and defect formation predictions. Additionally, interfacial interactions, substrate-induced strains, and chemical environment alterations during deposition and annealing must be considered. To facilitate new amorphous material engineering, the introduction of novel approaches is thus necessary to map density dependencies and material evolutions over large energy and density landscapes.

Molecular dynamics (MD) simulations, traditionally used for exploring PES by simulated annealing, face challenges in capturing long-lived metastable states [5] due to limited accessible timescales in typical nanosecond ranges. The nudged elastic band (NEB) technique [6], an alternative approach, requires prior knowledge of local minima positions and extensive computations that needs to be validated [7]. Elaborated methods to explore high-dimensional random PES, such as stochastic surface walking [8], anharmonic downward distortions [9], meta/hyper-dynamics [10], umbrella sampling [11], have limitations in capturing rare events and exploring large conformational spaces due to their reliance on prior knowledge of bias and predefined cumulative or collective variables to guide the simulation

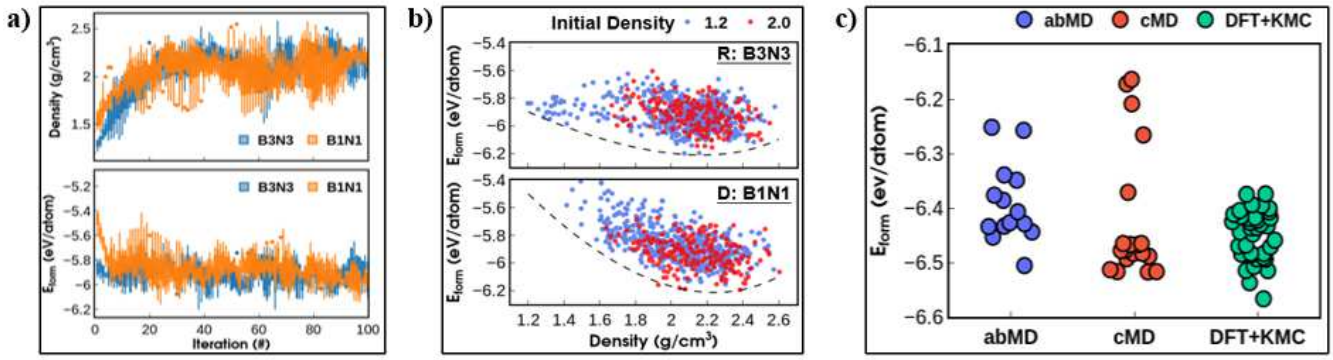

Fig. 2. a) Density and E_{form} evolution along DFT+KMC iterations for B_3N_3 and B_1N_1 fragments. b). E_{form} vs density correlation for 1000 aBN structures obtained with variable initial densities and fragment distributions by DFT+KMC. c) Enhanced structural stability is achieved by DFT+KMC over abMD, cMD methods.

towards specific regions of the PES. Recent developments in machine learning (ML) [12-15], swarm-based optimization [16], and genetic algorithms [17] hold promise for quick identification of metastable energy minima and transition states on PES, however optimization of these methods for amorphous systems requires generation of diverse and extensive training datasets to account for the absence of long-range order and the formation of diverse atomic network bonding characteristics.

II. OVERVIEW OF METHODS

To tackle the challenges above, a generally applicable, efficient unbiased method is introduced that can provide a comprehensive mapping of PES and the method is showcased for aBN low-k material engineering. The model involves pulse-like one-shot repeated structural perturbations of an amorphous structure by a kinetic Monte Carlo (KMC) step. QATK [18] and VASP packages [19-20] were used for the DFT+KMC and k value calculations, and PES mapping was benchmarked against MD, *ab initio* (abMD) and classical (cMD) using a Tersoff force field [21-22]. Within DFT+KMC the repetitive perturbation pulses are applied to partially converged systems to prevent local minima trapping (Fig. 1), then intermediate low energy structures with varying densities are extracted and fully optimized to assess metastability. The electronic contributions to k values calculated using high-precision HSE [23] and RPA [24] approximations are compared to high frequency experiments. DFT+KMC shows a 1.5x improvement in computation time compared to cMD due to efficient and continuous energy-density mapping. In near future, to further speed up amorphous landscape mapping, it is envisioned the use of this technique with powerful graph neural ML interatomic potentials that exhibit DFT accuracy.

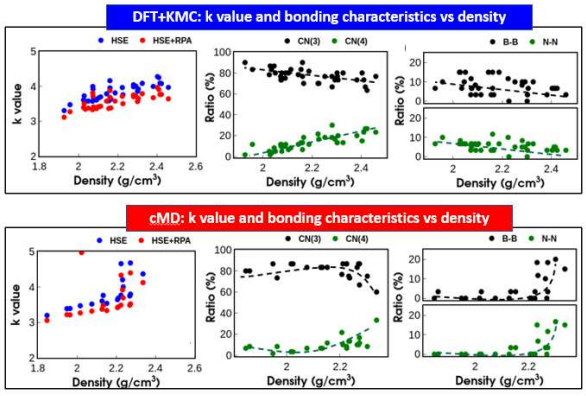

Fig. 3. k value, CN(3)/CN(4) coordination and B-B/N-N bond ratio vs density analysis with HSE and HSE + RPA methods.

III. RESULTS AND DISCUSSIONS

a. aBN structure derivation and benchmarking

Using B3N3 and B1N1 randomly placed fragments derived from B3N3H6 and BNH6 precursors commonly used in aBN growing experiments, the energy-density space exploration with two initial densities (1.2 g/cm3 and 2 g/cm3) yielded multiple metastable structures with low formation energies (E_{form}) at densities ~ 2.2 g/cm3, close to experimental values [8-9], demonstrating the robustness of DFT+KMC method. Structure evolution showed quick rough equilibration within 20 iterations for 5 samples, for both density and E_{form} as shown in Fig. 2b), allowing efficient statistics derivation

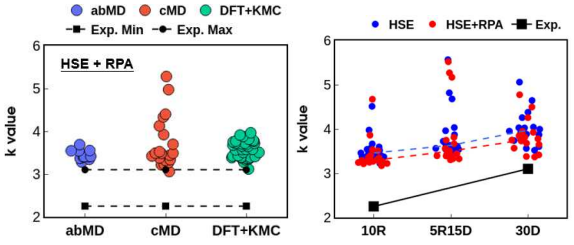

Fig. 4. Validation with experiments: k values by DFT+KMC reach the exp. max value. Lower k-values were obtained for ring-shaped (R: B6N6) precursor fragments over dimers (D: B1N1), in agreement with experimental trend.

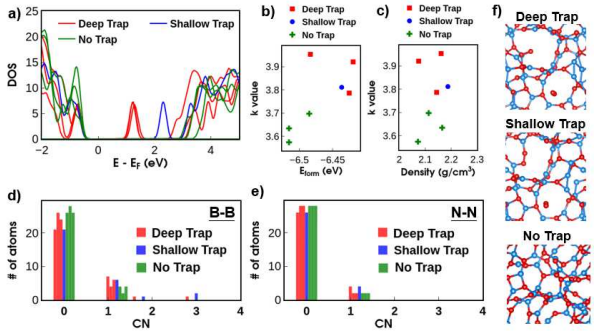

Fig. 5. a) Density of states (DOS) of structures exhibiting distinctive deep and shallow trap states at similar density. b) k value is found to be strongly affected by the nature of traps and their energies. c) and d) B-B and N-N defects are shown to induce more trap states. e) Depiction of local atomic environments for deep, shallow and no defect cases.

from the remaining structures. Method validation regarding stability, i.e., low E_{form} of metastable structures, indicate that abMD and cMD show larger energy dispersions over DFT+KMC, Fig. 2c) and therefore are less efficient in mapping the PES. The averaged radial distribution g(r) functions demonstrate good amorphous film quality (Fig. 1), with first peaks at $r_{abMD} = 1.53$ Å, and $r_{cMD} \cong r_{DFT+KMC} = 1.48$ Å, in agreement with previously reported values [1, 25].

b. aBN density correlation to k value

In the quest to establish k value and bonding characteristics trends, aBN structures analysis yields a direct correlation between k value and density, which is supported by: i) limited void space; ii) bond type changes from sp2 to sp3, characterized by atomic coordination trends of CN(3) and CN(4), as depicted in Fig. 3. The unusual upturn in k value with density observed in cMD is attributed to increased number of homonuclear bonds formation and B-B/N-N clustering/segregation.

c. Theoretical aBN k value vs experimental results

The theoretical k value distributions calculated with accurate HSE and RPA approximations for aBN structures, Fig. 4, are shown to reach the experimental processing window. Moreover, k value dependence on initial precursor fragment type matches the experimental trend [1], i.e. aBN built from BN dimers tend to consistently have higher k values over rings.

d. Amorphous bandgap and trap effects on k value

k values are known to inversely correlate with the bandgap, however the additional tail states in amorphous materials, segregation issues and partially bonded atoms in porous region further complicate the picture. Getting access to multiple metastable coexisting configurations in an amorphous matrix by employing the DFT+KMC method, on the fly statistical analysis becomes possible for all the above-mentioned effects. From Fig 5a), systems with either deep or shallow trap levels tend to induce higher k values at similar

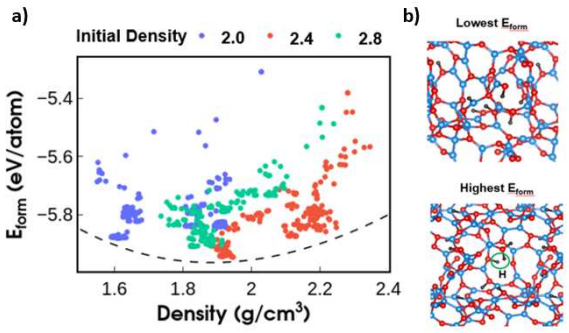

Fig. 6. a) E_{form} vs density for 1000 aBN+10 % H derived from variable initial density structures. b) Atomic arrangements corresponding to high/low E_{form}.

densities as defect-free cases as shown in Fig 5c). The formation of B-B and N-N homonuclear bonds are identified to be responsible for these effects, Fig. 5d),e), i.e. deep and shallow traps originate from dangling bonds of atoms located near porous regions as shown in the atomic configurations depicted in Fig. 15f).

e. Hydrogen impurity effects on aBN structure evolution

With the vast transferability of DFT+KMC, additional impurities can be straightforwardly added to study their effects on aBN formation density and evolution. Starting from 3 different initial densities of 10% H containing random fragment configurations, general density lowering trends relative to pristine aBN are observed, 1.9 g/cm^3 vs 2.2 g/cm^3, Fig. 6a). The structures with lowest/highest E_{form} are shown in Fig. 6b), and the corresponding charge distribution differences indicate that H incorporation mechanism into aBN consists of: i) preference for porous regions; ii) binding to partially bonded B; iii) effective pore sizes reduction from ~4.3 Å to ~3 Å (Fig. 7a),b)). Average porosities of aBN with and without H are found to be in a similar range (Fig. 8a)), even though the hydrogenated samples exhibit lower densities and smaller individual pore sizes. Given the average porosity correlation to k value established for aBN (Fig. 8b)) it is predicted that H:aBN samples will possibly attain similar k values. This projection was verified for a few H:aBN cases

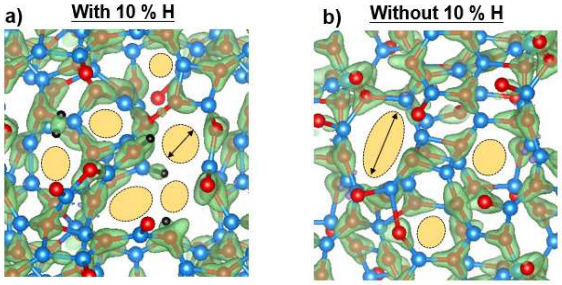

Fig. 7. Atomic charge differences in samples with a) and without b) 10 % H, the porosity ~ 0.25 is found to have distinctive distributions as indicated by yellow ellipses. Mean pore sizes are ~ 3 Å with 10% H inclusion, while ~ 4.3 Å for samples with no H.

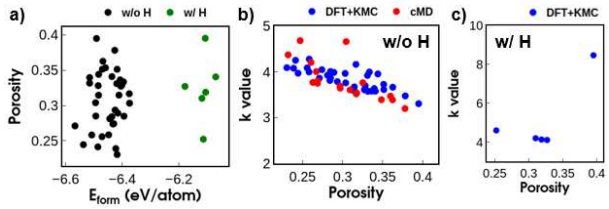

Fig. 8. a) Comparison of porosities in structures with and without H vs E_{form} b) k values vs porosity of aBN structures without H content calculated from DFT+KMC and cMD methods. c) k value vs porosity of aBN structures containing H.

and shown to follow the predicted trend in Fig.8(c), nevertheless more sampling will be needed in the future to reach a more general conclusion.

IV. SUMMARY AND OUTLOOK

A novel, efficient, and general simulation approach based on quantum mechanical simulations was put forward that accelerates amorphous density-energy landscape mapping and material characterization. The model is validated by a comprehensive study of aBN and k value results are found to agree well with experimental findings. Furthermore, previously unreachable insights into factors affecting k value engineering were obtained by in debt atomistic analysis of segregation trends, tail states and trap levels, and H impurity induced effects.

ACKNOWLEDGEMENTS

The authors acknowledge the experimental team for providing measured data and for in-debt discussions C.-M. Lin, W.Y. Woon and S. Liao.

REFERENCES

[1] C.-M. Lin , C.-H. Hsu , W.-Y. Huang , V. Astié , P.-H. Cheng , Y.-M. Lin , W.-S. Hu , S.-H. Chen , H.-Y. Lin , M.-Y. Li , B. Magyari-Köpe , C.-M. Yang , J.-M. Decams , T.-L. Lee , D. Gui , H. Wang , W.-Y. Woon , P. Lin , J. Wu , J.-J. Lee , S. S. Liao and M. Cao , "Ultralow-k amorphous boron nitride based on hexagonal ring stacking framework for 300 mm silicon technology platform", *Adv. Mater. Technol.*, 2200022, (2022).

[2] S. Hong, C.-S. Lee, M.-H. Lee, Y. Lee, K. Y. Ma, G. Kim, S. I. Yoon, K. Ihm, K.-J. Kim, T. J. Shin, S. W. Kim, E.-C. Jeon, H. Jeon, J.-Y. Kim, H.-I. Lee, Z. Lee, A. Antidormi, S. Roche, M. Chhowalla, H.-J. Shin, H. S. Shin, "Ultralow-dielectric-constant amorphous boron nitride", *Nature*, 582, 511, (2020).

[3] L. Li and X. M. Chen, "On the measured dielectric constant of amorphous boron nitride", *Nature*, 590, E6, (2021).

[4] J. Wu and B. Magyari-Köpe, "Advances in atomistic modeling for predictive TCAD applications", *2021 International Conference on Simulation of Semiconductor Processes and Devices (SISPAD)* 48, (2021).

[5] D. Frenkel, D., & B. Smit, "Understanding molecular simulation: From algorithms to applications", *Academic Press.*, (2002).

[6] G. Henkelman and H. Jónsson, "Improved tangent estimate in the nudged elastic band method for finding minimum energy paths and saddle points", *J. Chem. Phys.*, 113, 9978, (2000).

[7] H. B. Schlegel, "Geometry optimization", *WIREs Comput. Mol. Sci.*, 1, 790, (2011).

[8] C. Shang and Z. P. Liu, "Stochastic surface walking method for structure prediction and pathway searching", *J. Chem. Theory Comput.*, 9, 1838, (2013).

[9] K. Ohno, Y. Osada, "Systematic Exploration of Chemical Structures and Reaction Pathways on the Quantum Chemical Potential Energy Surface by Means of the Anharmonic Downward Distortion Following Method", *Advances in the Theory of Quantum Systems in Chemistry and Physics*, vol 22. Springer, (2012).

[10] A. Laio, & M. Parrinello, "Escaping free-energy minima", *Proc. Natl. Acad. Sci.*, 99, 12562, (2002).

[11] T.B. Tan, A.J. Schultz, and D. A. Kofke "Suitability of umbrella- and overlap-sampling methods for calculation of solid-phase free energies by molecular simulation", *J. Chem. Phys.*, 132, 214103, (2010).

[12] J. Behler and M. Parrinello, "Generalized neural-network representation of high-dimensional potential-energy surfaces", *Phys. Rev. Lett.*, 98,146401, (2007).

[13] L. Zhang, J. Han, H. Wang, R. Car, and E. Weinan, "Deep potential molecular dynamics: a scalable model with the accuracy of quantum mechanics", *Phys. Rev. Lett.*, 120, 143001, (2018).

[14] L. Li, M. Agrawal, S.Y. Yeh, K.T. Lam, J. Wu, and B. Magyari-Köpe, "Towards accurate and efficient process simulations based on atomistic and neural network approaches", *IEDM Technical Digest*, (2022).

[15] O. Kaya, L. Colombo, A. Antidormi, M. Lanza and S. Roche, "Revealing the improved stability of amorphous boron-nitride upon carbon doping", *Nanoscale Horiz.*, 8, 361, (2023).

[16] C.L. Tsai and G.H. Fredrickson,"Using particle swarm optimization and self-consistent field theory to discover globally stable morphologies of block copolymers", *Macromolecules*, 55, 5249, (2022).

[17] A. R. Oganov and C. W. Glass, "Crystal structure prediction using ab initio evolutionary techniques: Principles and applications", *J. Chem. Phys.*, 124, 244704, (2006).

[18] S. Smidstrup, T. Markussen, P. Vancraeyveld, J. Wellendorff, J. Schneider, T. Gunst, B. Verstichel, D. Stradi, P.A. Khomyakov, U.G.Vej-Hansen, M.E. Lee, S.T. Chill, F. Rasmussen, G. Penazzi, F. Corsetti, A. Ojanperä, K. Jensen, M. L.N. Palsgaard, U. Martinez, A. Blom, M. Brandbyge, K. Stokbro , "QuantumATK: an integrated platform of electronic and atomic-scale modelling tools", *J. Phys. Condens. Matter*, 32, p.015901, (2020).

[19] G. Kresse and J. Hafner, "*Ab initio* molecular dynamics for liquid metals", *Phys. Rev. B*, 47, 558, (1993); *ibid.* 49, 14251 (1994).

[20] G. Kresse and J. Furthmüller, "Efficient iterative schemes for *ab initio* total-energy calculations using a plane-wave basis set", *Phys. Rev. B*, 54, 11169, (1996).

[21] K. Matsunaga and Y. Iwamoto, "Molecular dynamics study of atomic structure and diffusion behavior in amorphous silicon nitride containing boron", *J. American Ceramic Society*, 84, 2213, (2001).

[22] K. Matsunaga, C.A.J. Fisher, H. Matsubara, "Tersoff potential parameters simulation cubic boron carbonitrides", *J. J. Appl. Phys.*, 39, (2000).

[23] J. Heyd, G. Scuseria, and M. Ernzerhof "Hybrid functionals based on a screened Coulomb potential", *J. Chem. Phys.*, 118, 8207, (2003).

[24] J. Paier, M. Marsman, and G. Kresse, "Dielectric properties and excitons for extended systems from hybrid functionals", *Phys. Rev. B*, 78, 121201, (2008).

[25] A. Antidormi, L. Colombo, and S. Roche, "Emerging properties of non-crystalline phases of graphene and boron nitride-based materials", *Nano Mat. Sci.*, 10, (2022).